Dielectric and polarization measurements on $BaTiO_3$ at high pressures to the tricritical point

D. L. Decker and Y. X. Zhao
Department of Physics, Brigham Young University, Provo, Utah 84602
(Received 1 August 1988)

Dielectric and polarization measurements were made on single crystal $BaTiO_3$ in a hydrostatic medium to 38 kbar. The nature of the ferroelectric phase transition is observed to go from first to second order near 35 kbar and -40 °C. The pressure–temperature–electric-field phase diagram of $BaTiO_3$ is measured. The tricritical point is indicated in this part of the phase diagram by a change in shape of both the real and imaginary parts of the dielectric response as the material passes through the cubic to tetragonal phase transition in zero electric field and by the pressure dependence of the critical points at the ends of the paraelectric-to-ferroelectric phase lines.

INTRODUCTION

At pressures below 40 kbar, $BaTiO_3$ is cubic at higher temperatures, but it undergoes a phase transition to a tetragonal phase with a small elongation of the c axis as the temperature is lowered. In the cubic phase the oxygens are centered on the six faces of a cubic cell with barium atoms at the corners and titanium at the body center of the cell. Below the transition temperature one of the cubic axes is stretched slightly (less than 1%) and the cell defined by the barium atoms becomes tetragonal, with the titanium atoms shifted off the body center along the tetragonal axis and the oxygen atoms displaced from the face centers in the opposite direction. Since the titanium and oxygen have opposite electrical charges, a dipole moment is set up and the tetragonal phase is ferroelectric with a spontaneous polarization along the c axis. More detail of this transition is given in Jona and Shirane.[1] This phase transition (near 130 °C for a pure melt-grown crystal at ambient pressure) is first order. However, it has been conjectured for several years that this phase transition in $BaTiO_3$ would change from first to second order at high enough pressure.[2,3] Such a point would be called a tricritical point.

Early pressure studies on this material[3] demonstrated that the transition temperature diminishes with pressure and that the peak of the dielectric constant anomaly increases with pressure. This latter result led to the prediction that the transition was approaching a continuous transition as the pressure was increased. Clark and Benguigui[4] measured the dielectric constant of a $BaTiO_3$ crystal in a nonhydrostatic pressure cell, and although the transition region became very broad, they reported a tricritical point at 34 kbar and 18 °C. They also followed the phase line to that pressure. Unfortunately the nonhydrostatic environment not only broadens the transition but also greatly alters the phase transition temperature, and may have some important effects on the interpretation of their results. The strong effects of nonhydrostatic pressures are likely due to the fact that the ferroelectric moment which appears in the low-temperature phase is accompanied by a ferroelastic spontaneous strain along the c axis. Decker and Pai[5] predicted from their dielectric measurements under a dc bias at elevated pressures that the transition would change to second order at 34 kbar and -45 °C for a flux-grown sample subject to hydrostatic pressure. A tricritical point is inferred in $PbTiO_3$, which has the same structure as $BaTiO_3$, because the transition is first order at atmospheric pressure and 492 °C, but appears to be second order at ambient temperature and 121 kbar.[6]

If a tricritical point exists in a simple structural phase transition such as the pyrovskite $BaTiO_3$, it would be an ideal system for experimentally examining the details of critical phenomena in the neighborhood of a tricritical point. We therefore undertook the task of repeating the measurement of the dielectric properties of $BaTiO_3$ near its ferroelectric phase transition as a function of pressure in a hydrostatic pressure environment.

The full theory of this transition with its long-range dipole interactions has not yet appeared. Devanshire[7] developed a mean-field theory of $BaTiO_3$ in its several phases. Clark and Benguigui[4] discuss the influence of a tricritical point on the mean-field theory of the transition. If one assumes a monodomain crystal of $BaTiO_3$ in the ferroelectric phase with order parameter η and expands the free energy in a power series of η, one gets

$$F=F_0+\tfrac{1}{2}A\eta^2+\tfrac{1}{4}B\eta^4+\tfrac{1}{6}C\eta^6 \ . \tag{1}$$

For stability the coefficient C must be positive at all pressures and temperatures while the coefficient $A(P,T)=0$ defines the stability limit in pressure-temperature space of the paraelectric phase and $B(P,T)=0$ separates the region where the transition is continuous from that where it is discontinuous. Thus if $A=0$ and $B>0$ the transition is second order but if $A=0$ and $B<0$ the transition is first order and $A=B=0$ defines the tricritical point. This is discussed further by Decker.[8] Since the order parameter in $BaTiO_3$ is proportional to the spontaneous polarization, we follow the thermodynamic approach of Devanshire using an expression for the free energy, includ-

ing the strain as well as the order parameter in the expansion. This gives $F(x,\eta)$, where x is the strain, and after a transformation similar to that of Forsbergh[9] one has $F(X,\eta)$, where X is the stress. The parameters in these expansions are functions of temperature. Assuming a monodomain crystal in a hydrostatic pressure P, where only one component of the order parameter is nonzero and all compressive stress components are equal to $P/3$, we then calculate the electric field $E(P,\eta)=\partial F(P,\eta)/\partial\eta$ and the inverse dielectric susceptibility $\chi^{-1}(P,\eta)=\partial^2 F(P,\eta)/\partial\eta^2$.

In the neighborhood of the ferroelectric phase transition of $BaTiO_3$ we have measured the dielectric constant versus pressure and temperature from 150 to -60 °C, and to 38 kbar. From these measurements and the theoretical expression for the susceptibility we have determined the inverse susceptibility function of temperature and pressure. We have also accomplished ferroelectric hysteresis measurements in this range of pressure and temperature to determine the polarization. From these latter measurements we show the existence of a tricritical point. A preliminary partial presentation of these measurements has appeared in the literature.[10] We first discuss the susceptibility measurements followed by the polarization measurements.

SUSCEPTIBILITY

Dielectric measurements

We have examined samples from several sources: flux-grown "butterfly" material from Samara, Nemelka, and Cleveland Crystal, and a small end from a melt-grown crystal from Linz. The best of the flux-grown material was from Cleveland Crystal and had a large dielectric peak at the transition near 124 °C and atmospheric pressure, and a sharp polarization hysteresis pattern. The melt-grown crystal had no region free enough of strain that we could pole it. It would not saturate in polarization studies to 10 kV/cm. It did give good dielectric constant measurements and showed a sharp discontinuity at the transition near 134 °C at atmospheric pressure. The magnitude of the discontinuity increased with increasing pressure. From c-domain regions of the flux-grown samples we cut 2-mm square sections with a wire saw. They were about 0.3 mm thick. They were etched lightly with phosphoric acid above the transition temperature before evaporating gold electrodes on the larger surfaces. Samples of about this same size were cut from the melt-grown material which were then polished, etched, and electroded.

The pressure system was a 400-ton hexahedral press. The six anvils press on the faces of a 25-mm on edge pyrophyllite cube into which was placed a 6.4-mm-diameter by 20-mm-long chamber containing the sample in a liquid environment as shown in Fig. 1. The electrical leads came out through the gaskets formed on pressing the cube. Petroleum ether was used as the pressure transmitting fluid in the chamber. The temperature was measured with a chromel-alumel thermocouple and the pressure was monitored with the resistance of a 100-Ω manganin wire of 0.02 mm diameter. The dielectric constant measurements were accomplished by measuring the capacitance of the sample with a Hewlett-Packard HP4274A LCR meter at 10 kHz and 0.1 V peak to peak. It was noted that the manner of attaching the electrical contacts to the electrodes was vital in preserving the sharpness of the transition. Contacts of very small wires attached with silver epoxy proved to be unsatisfactory because this badly strained the crystal under pressure, as evidenced by broadening of the transition even when pains were taken to use very small amounts of epoxy. We thus developed a mechanical contact shown in Fig. 1 with gold-plated bellows making the electrical contact to the electroded $BaTiO_3$ surface. The capacitance data, the thermocouple emf, and the manganin resistance were all fed to a Hewlett Packard HP9825A desk computer where the data were analyzed and plotted. The dielectric measurements were made either by slowly varying the temperature at constant press load and monitoring the pres-

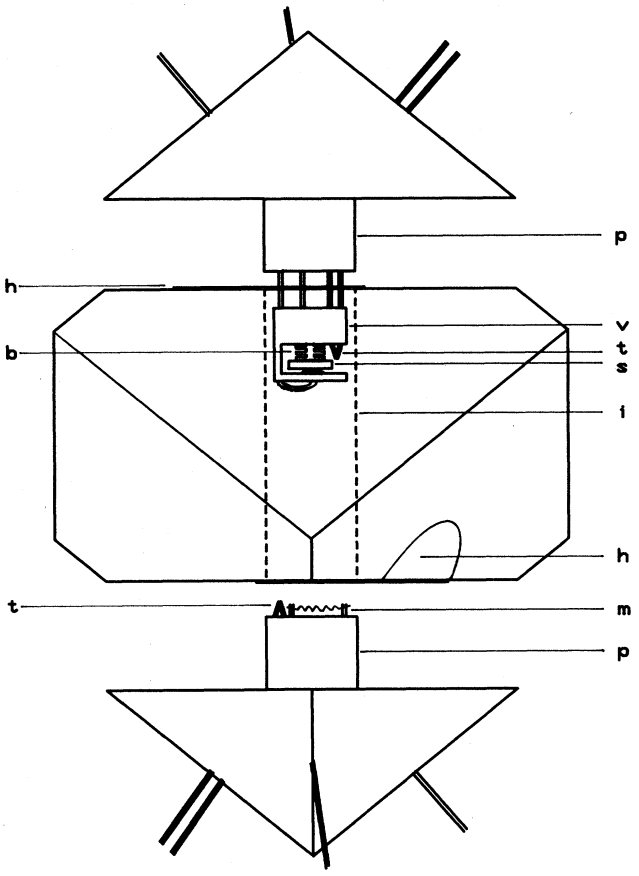

FIG. 1. The sample cell used in the cubic multianvil press with the axis of the cell along the body diagonal of the cube. *p*, polyethylene plug, *v*, vespel high-temperature plastic, *t*, chromel-alumel thermocouple junction, *s*, $BaTiO_3$ sample, *h*, heating tab to pass current through the inconel tube, *b*, gold plated bellows, *i*, thin-wall inconel tube filled with petroleum ether, *m*, manganin coil.

sure, temperature, and both the real and imaginary components of the capacitance as the transition was traversed, or by slowly varying the press load at constant temperature, again monitoring the appropriate parameters. Stray capacitance, which was less than 1 pF compared to sample capacitances greater than 300 pF, was zeroed out after the press rams crushed the pyrophyllite. There was negligible change in stray capacitance thereafter, for there was little change in physical dimensions. The accuracy of the pressure at higher or lower temperatures is only about ± 1 kbar because of temperature effects on the manganin resistance, which were only partially compensated for; but the sensitivity is of the order of a bar. There is an increase or decrease in the sample pressure when heating or cooling the sample chamber at constant press load because of thermal expansion of the sample and its surroundings against the anvil faces.

Results and Analysis

In Fig. 2 we show the variation of the dielectric constant calculated from the measured capacitance, and the loss factor versus pressure through the ferroelectric phase transition at 24 °C. The phase transition at this temperature appears at 20 kbar, as seen in the figure. In Fig. 3 we show a collection of dielectric measurements, i.e., real and imaginary components of the dielectric constant, at constant load versus temperature. The pressure in kilobars, indicated on each curve, is that at the transition. One observes the growth in the height of the dielectric anomaly and a change in the nature of the loss factor on the low-temperature side of the transition as the tricritical point is approached. A strong dielectric loss appears on the ferroelectric side of the transition as one gets close to the critical region. We find no theoretical analysis of this loss component in the literature. In Fig. 4 we show χ^{-1} at constant load versus temperature for both flux-grown and melt-grown samples. For the flux-grown sample the changeover from first to second order in the tran-

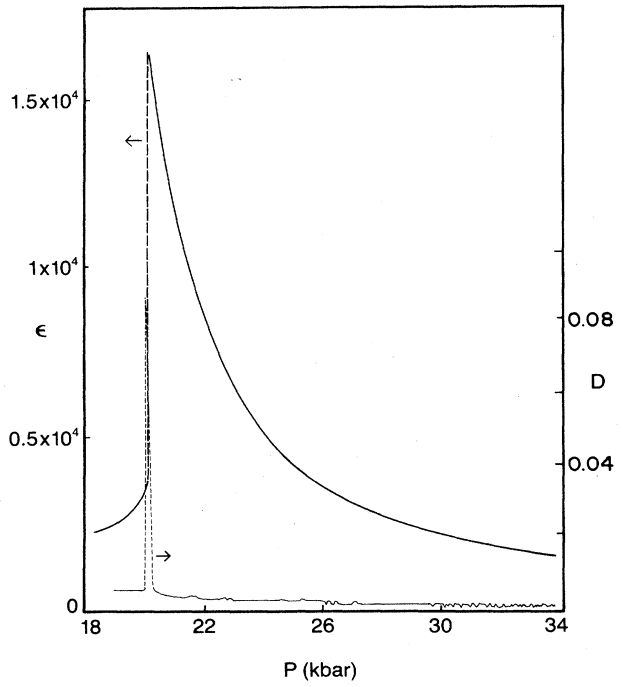

FIG. 2. The real part of the dielectric constant ϵ and the loss factor D from the out-of-phase response vs pressure at 24 °C.

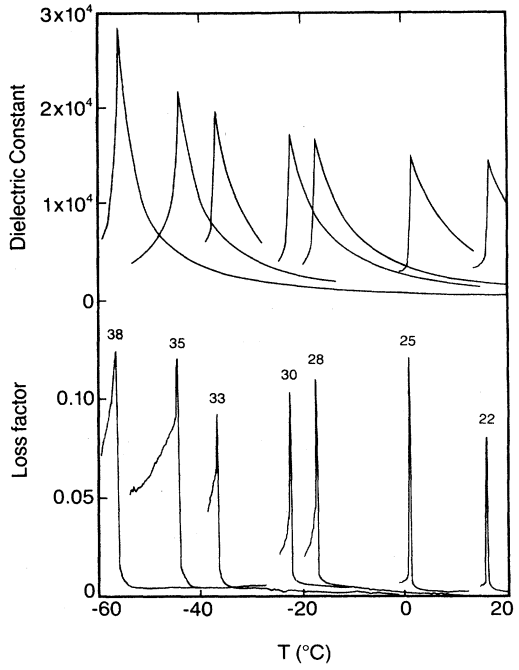

FIG. 3. The loss factor D and dielectric constant ϵ vs temperature at several selected press loads. The numbers indicate the pressure in kbar at each ferroelectric transition.

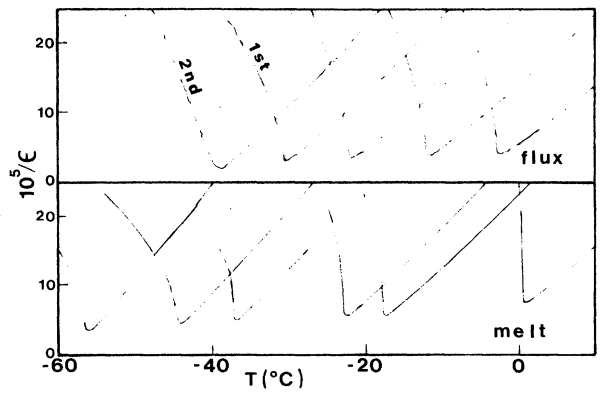

FIG. 4. Inverse electric susceptibility vs temperature at several selected press loads for a flux-grown and a melt-grown sample. The change from first-order to second-order transition is indicated in the data for the flux-grown crystal.

sition is related to a change from negative to positive curvature on the ferroelectric side of the transition as indicated in the figure near $-40\,^{\circ}\mathrm{C}$. For the flux-grown material this transition is at lower temperatures approximately $-50\,^{\circ}\mathrm{C}$.

An analysis of the inverse susceptibility on the paraelectric side of the phase transition can yield a function for the pressure and temperature dependence of this quantity. Before doing this analysis, however, one must determine the form of the inverse susceptibility function. This inverse susceptibility, in the paraelectric phase ($\eta=0$) with no applied electric field determined from $\partial^2 F(P,\eta)/\partial\eta^2$, as discussed above, is

$$\chi^{-1}=A+KP+LP^2 . \tag{2}$$

These are the first few terms of an expansion in pressure in which the coefficients A, K, and L can be functions of temperature.

It has been observed at zero pressure that the inverse dielectric constant in the paraelectric phase is linear in temperature near the transition. Since there is nothing unique about any certain pressure we assume that χ^{-1} is linear in T at all pressures. Equation (2) indicates that at constant temperature in the paraelectric phase χ^{-1} could be nonlinear in pressure. Furthermore, our measurements indicate that the stability limit boundary, $T_0(P)$, is linear in P to within experimental error. We form an empirical model consistent with all these concepts by referring to Fig. 5. We write,

$$T_0=T_{00}-mP \tag{3}$$

and

$$\chi^{-1}=(A_0+aP)(T-T_{00}+mP) , \tag{4}$$

where all temperature and pressure dependence is explicitly shown. A_0 and a are parameters to be evaluated experimentally, while $-m$ is the slope of the stability limit line and T_{00} is the intercept of the stability line at zero pressure. Note that at constant pressure χ^{-1} is linear in T going to zero at $T=T_0(P)$, but at constant temperature χ^{-1} varies quadratically with pressure. As explained in the preceding section, increasing the temperature of the sample while keeping a constant press load will result in an increase in the internal pressure. Therefore the inverse susceptibility data taken at constant press load will vary quadratically with temperature as indicated in Fig. 5.

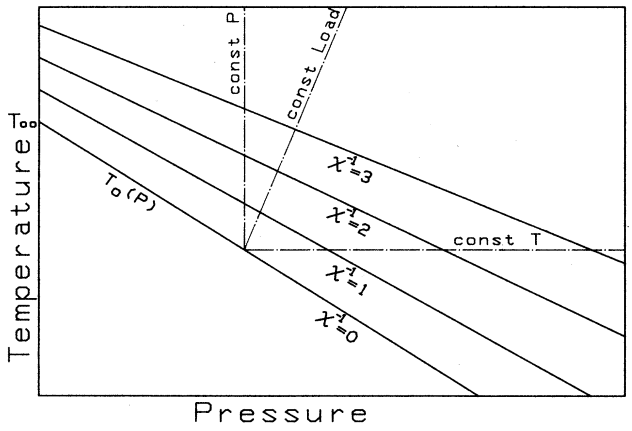

FIG. 5. Model, consistent with experimental data, for calculation of the pressure and temperature dependence of the electric susceptibility in the paraelectric phase near a critical point. Lines of constant χ^{-1} in arbitrary units are shown. Also shown are the paths of the measurements at constant temperature and constant load. $T_0(P)$ is the stability limit of the paraelectric phase.

The dielectric constant data were analyzed from measurements of χ^{-1} versus pressure at constant temperature in the paraelectric state (these were analyzed by fitting to a quadratic function of pressure) or from χ^{-1} versus temperature at constant load in the paraelectric state (these were analyzed by fitting to a quadratic function of temperature as already discussed). In the analysis one must also consider the following two points: (1) There is a nearly temperature- and pressure-independent contribution to the susceptibility which does not arise from the soft-mode response. (2) There are some effects principally due to surface defects that limit the dielectric constant from going infinite even in a second-order phase change.

Let the sample be of thickness t with a background dielectric constant χ_0 and a soft-mode dielectric susceptibility χ_s active over all but a surface layer of thickness t', then assuming the capacitance of the crystal to arise from that of two surface regions and the central section all in series one finds, after some computation, the measured or effective susceptibility to be

$$\chi^{-1}=(\chi_s^{-1}+2\tau/\chi_0)/(1+\chi_s^{-1}\chi_0) , \tag{5}$$

where $\tau\equiv t'/t$.

Assuming $\tau\ll 1$ and $\chi_s\gg\chi_0$ Eq. (5) becomes

$$\chi^{-1}=2\tau/\chi_0+\chi_s^{-1}-\chi_0\chi_s^{-2} . \tag{6}$$

Now returning to our model, Eq. (4) represents the soft-mode susceptibility, and with some algebra one can cast it in the form for constant temperature T:

$$\chi_s^{-1}=[A_0m+a(T_{00}-T)]p+amp^2 , \tag{7}$$

where $p\equiv P-P_0$, with P_0 satisfying the equation $T=T_{00}-mP_0$. While at constant load the corresponding equation is of the form

$$\chi_s^{-1}=(A_0+aP_0)(1+mS)t+aS(1+mS)t^2 , \tag{8}$$

where $t\equiv T-T_0$ and $P-P_0=S(T-T_0)$ gives the pressure increase due to thermal expansion as the temperature is increased. We substitute Eqs. (7) or (8) into (6) to get the appropriate expressions for the measured susceptibilities in these two types of experiments. In each case one finds a quadratic function in either pressure or temperature.

From measurements of the dielectric constant far from the transition we assume $\chi_0=10$ and from the peak value of the susceptibility at the second-order transition we assume $2\tau/\chi_s=158\,000$. We are using cgs units with the

susceptibility being dimensionless. The value of S has been determined from other experiments in our laboratory to be 16 bars/deg.[11] From the coefficients determined by the least-squares fitting of the experimental data to the appropriate quadratic function we then get values of the parameters $A_0 = 1.35 \times 10^{-6}$ deg^{-1}, $m = 5.16$ deg/kbar, $T_{00} = 115.6$ °C, and $a = 1.8 \times 10^{-7}$ deg^{-1} kbar^{-1}. Putting these results into Eq. (4) one has the temperature and pressure dependence of the susceptibility in the cubic phase of $BaTiO_3$. These results are for the flux-grown crystal from Cleveland Crystal.

POLARIZATION

Polarization measurement

The high-pressure polarization measurement is the same as that described by Decker[8] at atmospheric pressure. The samples and high-pressure cell are the same as those described for the measurement of susceptibility. The hysteresis patterns of polarization versus applied electric field were traversed in 50 s while the pressure and temperature remained constant. The circuit is shown in Fig. 6 with the compensation circuit in a dashed line. The physical circuit did not contain the compensation section but consisted of a high-quality operational amplifier and a computer programmed to calculate from the measured hysteresis patterns after each cycle an effective resistance and capacitance of the shown compensation circuit and to center the polarization about zero. Several cycles were traversed, each time recalculating the compensating R and C, until there was no change in the calculated parameters.

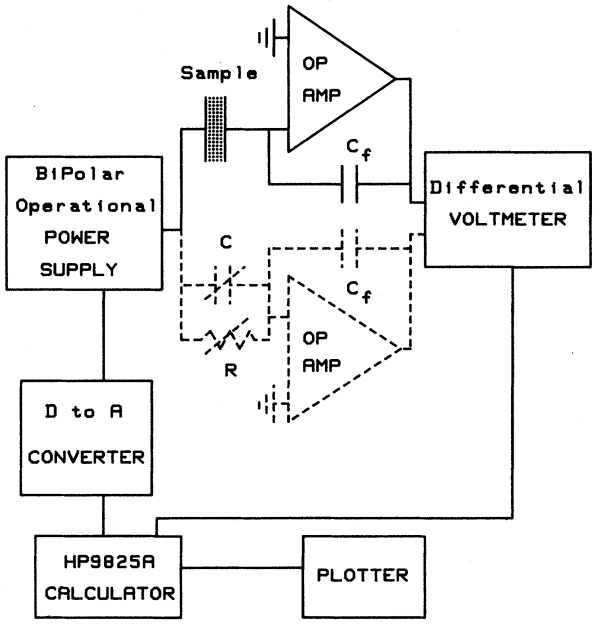

FIG. 6. Polarization measurement circuit. The circuit shown by a dashed line was not physically present, but its output for a given compensating capacitance C and resistance R was calculated by the computer and subtracted from the measured signal generated by the sample.

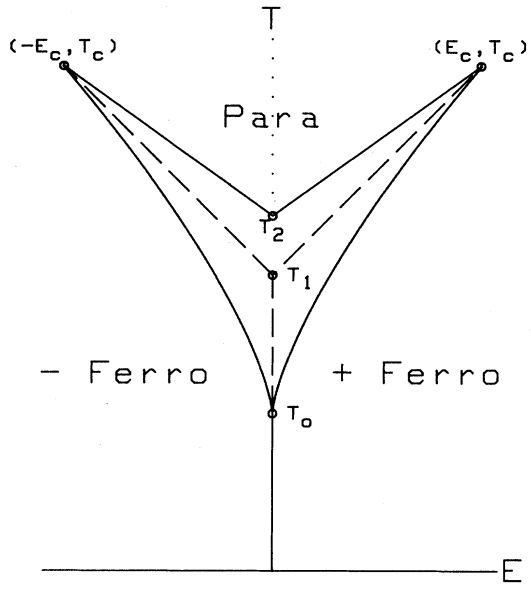

FIG. 7. A temperature T and electric field E plane of the phase diagram of $BaTiO_3$. (E_c, T_c) indicate the critical points, Para the paraelectric phase, +Ferro and −Ferro are two different polarizations of the ferroelectric phase. T_0 is the limit of stability of the paraelectric phase, T_1 the equilibrium temperature of the phase change, and T_2 the stability limit of the ferroelectric phase.

Analysis and results

In Fig. 7 we show a constant pressure cross section of the pressure–temperature–electric-field phase diagram.[12] In this temperature versus electric-field plane the positively and negatively polarized ferroelectric phases are below the ferroelectric phase transitions represented by the lines from T_1 to T_c. They are separated from each other by a first-order phase line along the $E = 0$ axis below T_0. The paraelectric phase is stable at temperatures above the first-order ferroelectric phase transitions which end in critical points (E_c, T_c). The lines T_0 to T_c are the limiting lines for the paraelectric phase while the lines T_2 to T_c form the boundary limiting the existence of the ferroelectric phase. A double hysteresis is observed when the temperature is such that sweeping the electric field causes the sample to cross the two first-order lines between T_1 and T_c, which we refer to as "wings." At temperatures above T_c no hysteresis is observed; however, the polarization versus electric-field curves are still strongly affected by the critical phenomena as evidenced by nonlinearity. Below T_0 a normal hysteresis pattern will be observed. Our measurements yielded hysteresis patterns of polarization versus applied external electric field. Typical hysteresis patterns are shown in Fig. 8 at several temperatures near the ferroelectric phase transi-

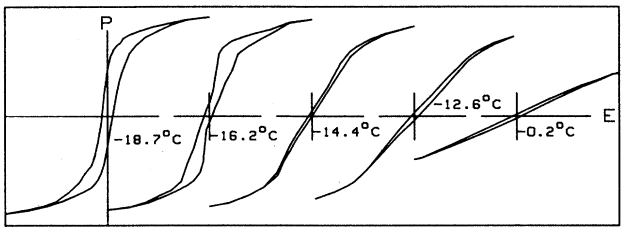

FIG. 8. Polarization vs applied electric field at 30.3 kbar and several selected temperatures as indicated on the figure.

tion at 30.3 kbar. Below the transition temperature, $-17.2\,^{\circ}\mathrm{C}$ at this pressure, a single hysteresis is observed upon sweeping the field. Above the transition a double hysteresis is evident until the temperature is above the critical point at the end of the wings, $-15.2\,^{\circ}\mathrm{C}$ at this pressure.

An idealized double hysteresis pattern is shown in Fig. 9 where the transition field E_t and wing polarization P_w are defined. At each pressure hysteresis patterns were measured at various temperatures in the range where double hysteresis patterns will appear. We analyzed these patterns for each set of data by measuring from the graphs P_w and E_t at each temperature. These quantities were plotted versus temperature for each set of data as shown in Fig. 10. The critical temperature T_c is determined as the point where the extrapolation of P_w versus temperature intersects the temperature axis and the critical field E_c is then read off the extension of the graph of E_t at that T_c. The extrapolation of E_t to zero should give T_1. As is evident from Fig. 8, it is not always easy to identify E_c and P_w from the experimental hysteresis patterns, so there is considerable uncertainty in the determination of E_c. Data similar to that in Fig. 10 were taken at several pressures, and the results of E_c and T_c versus pressure are plotted in Fig. 11. In spite of the uncertainty in the measurement, a definite pressure dependence of E_c is clearly evident, as shown by the results in Fig. 11. It is noted that the field at the critical point is decreasing to zero as the pressure increases. When this field goes to zero the critical point at the ends of the two wings of the transition have converged to a tricritical point and form a second-order phase line in the temperature-pressure ($E=0$) plane beyond that point. The measured values of T_c then extrapolate to a tricritical point of $-40\,^{\circ}\mathrm{C}$ with a critical pressure of 35 kbar. These data are for the flux-grown crystals. Since we could not make good hysteresis measurements using the melt-grown material, we could not get similar data to pin down the tricritical point for that type of material.

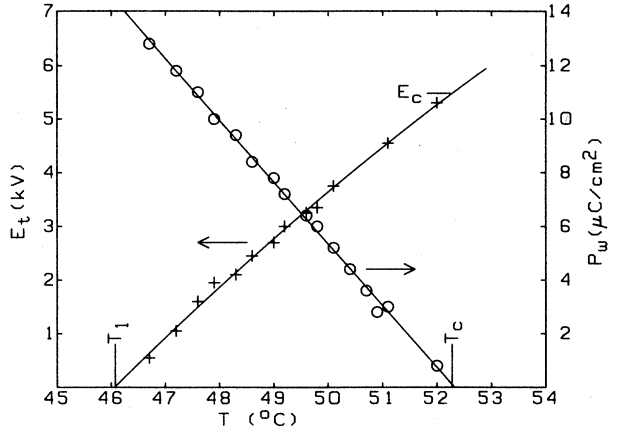

FIG. 10. The transition field E_t, and wing polarization P_w vs temperature for a measurement of 13.3 kbar. This plot demonstrated how to find T_1, T_c, and E_c at this pressure.

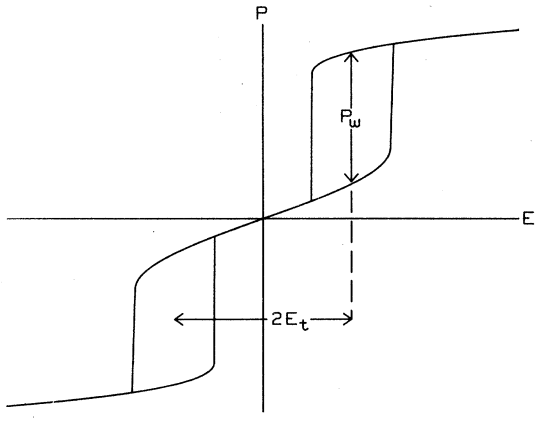

FIG. 9. An ideal double hysteresis pattern in which the transition field E_t and the wing polarization P_w are defined.

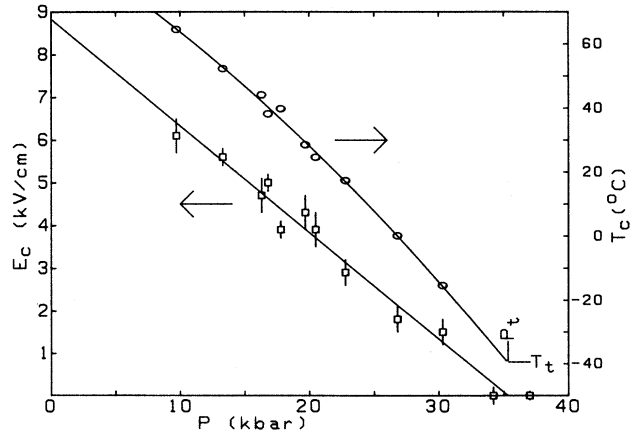

FIG. 11. The critical field E_c and critical temperature T_c vs pressure P. The point where E_c goes to zero is the tricritical point, with P_t and T_t the pressure and temperature at this point.

CONCLUSIONS

Under a hydrostatic pressure the $BaTiO_3$ ferroelectric phase transition is displacive and becomes less discontinuous as pressure is increased, until a tricritical point is reached at 35 kbar and $-40\,^{\circ}C$ for good flux-grown single crystals, and ~ 35 kbar and $\sim -50\,^{\circ}C$ for melt-grown single crystals. The evidence for the existence of this point comes first from the observed change in the shape of the curve of χ^{-1} versus T as one approaches the transition from below; second, from the loss-factor measurement, which shows a symmetrical soft-mode-generated loss on each side of the transition is the continuous phase transition; and third, an extrapolation of the measured critical electric field of the critical points at the end of the "wings" versus pressure. All of these measurements confirm the above conclusion. No theory of the imaginary component of the dielectric constant seems to be available for the critical region near a critical point where linear response theory is not sufficient. This would be a good theoretical problem.

ACKNOWLEDGMENTS

We wish to acknowledge the help of several who helped to develop techniques that made this work possible, such as Kuei-Fang Pai and Kathleen Olson Scott. We thank Dorian Hatch and Dean Barnett for their helpful discussion of this work.

[1]F. Jona and G. Shirane, *Ferroelectric Crystals* (Pergamon, Oxford, 1962), Chap. 4.

[2]I. N. Polandov, B. A. Strukov, and V. P. Mylov, Fiz. Tverd. Tela (Leningrad) **9**, 1477 (1967) [Sov. Phys.—Solid State **9**, 1153 (1967)].

[3]G. A. Samara, Ferroelectrics **2**, 277 (1971).

[4]R. Clarke and T. Benguigui, J. Phys. C **10**, 1963 (1977).

[5]D. L. Decker and K. F. Pai, Bull. Am. Phys. Soc. **26**, 476 (1981).

[6]J. A. Sanjurjo, E. Lopez-Cruz, and G. Burns, Solid State Commun. **48**, 221 (1983).

[7]A. F. Devonshire, Philos. Mag. **40**, 1040 (1949); **42**, 1065 (1951).

[8]D. L. Decker, Encyclia **58**, 102 (1981).

[9]P. W. Forsbergh, Jr., Phys. Rev. **93**, 686 (1954).

[10]D. L. Decker and Y. X. Zhao, in *High Pressure in Science and Technology*, edited by C. Homan, R. K. MaCrone, and E. Whalley (North-Holland, New York, 1984), Vol. 22, p. 179.

[11]D. L. Decker, J. D. Jorgensen, and R. W. Young, High Temp. High Pressures **7**, 331 (1975).

[12]R. B. Griffiths, Phys. Rev. Lett. **24**, 715 (1970).